**DOR: 20.1001.1.2322388.2021.9.2.3.1**

Research Paper

# Inclusion Removal Mechanisms of Al-Killed 304 Low Carbon Stainless Steel Melt Using Hercynite Coated $Al_2O_3$-C Ceramic Foam Filters

**Ali Baghaei[1], Amir Abbas Nourbakhsh[1,2]*, Reza Ebrahimi Kahrizsangi[1]**
*1. Advanced Materials Research Center, Materials Engineering Department, Najafabad Branch, Islamic Azad University, Najafabad, Iran*
*2. Department of Materials Science and Engineering, Shahreza Branch, Islamic Azad University, Shahreza, Iran*

## ARTICLE INFO

*Article history:*

Received 25 August 2020
Accepted 30 August 2020
Available online 1 May 2021

*Keywords:*
*$Al_2O_3$-C foam filters*
*Alumina*
*Refractories*
*Steel filtration*
*Carbon*

## ABSTRACT

Carbon bonded alumina foam filters have been successfully using for steel melt filtration. Enhancement of the filtration capacity of $Al_2O_3$-C foam filters is a key factor in order to make them applicable to be used for large steel casting parts or continuous casting of steel. In the present study, filtration performance of hercynite coated carbon bonded alumina foam filters containing 1 Wt.% of nano-$TiO_2$ were evaluated by the exposure to an Al-killed 304 low carbon stainless steel melt. Successful impingement of steel melt into the filters revealed the filter structure strength and effectiveness under casting temperature and molten metal exposure conditions. Microstructural investigations using a field emission scanning electron microscope (FESEM) equipped with energy dispersive X-ray spectroscopy (EDS) analysis of the active hercynite coated filter surfaces after steel melt filtration revealed the entrapment of the oxide inclusions from the steel melt on the surface of the filter. In addition, filtration mechanisms for whiskers and dendritic $Al_2O_3$, and hercynite inclusions at different Al/oxygen activity conditions of the steel melt were proposed. To this end, the feasible potential for the application of hercynite coated $Al_2O_3$-C filters for low and ultra-low carbon steel casting processes could be promising.

---

* **Corresponding Author**:
E-mail Address: anourbakhs@yahoo.com

## 1. Introduction

The presence of non-metallic inclusions (NMIs) in the steel melt drastically affects the properties of steel casting parts. In fact, the amount, type, shape, and distribution of solid NMIs in the steel castings decrease the fatigue and corrosion resistance as well as ductility and fracture toughness [1-5]. Consequently, improvement of steel cleanliness considers the application of steel refining systems. In this way, ceramic foam filters (CFFs) have been used in the steel industry for several decades in order to entrap NMIs from the molten steel and promote non-turbulent melt filling of the mold so as to reduce the possibility of metallic melt reoxidation [6-7].

Various production techniques have been used to manufacture reticulated ceramic foams, including the hollow beads method, foaming of slurries, robocasting of 3D structures, extrusion of cellular ceramic filters, and the polymeric sponge replica method. Among these techniques, the polymeric sponge replica method is the most common way to produce CFFs [8-12].

The application of $Al_2O_3$-C filters for the production of steel castings is of great interest due to their lower cost, higher filtration capacity, higher thermal shock and creep resistances, and high refractoriness compared to zirconia CFFs, which are currently the most common filter material for the steel melt filtration. [13].

Novel carbon bonded alumina CFFs have been successfully developed by Emmel and Aneziris [14] for the filtration of steel melts in order to produce efficient filters for longer casting operations. The proposed composition for the production of CFFs is based on 70wt.% $Al_2O_3$ and 30wt.% C sintered at 800ºC in reducing atmosphere.

In order to inhibit carbon pick up by the steel melt and influencing the wettability and the following improved deposition and adhesion behaviors of NMIs existing in the molten steel, some researchers [15-18] have developed filters with a modified surface. To this aim, active and reactive ceramic coatings have been applied on the surface of carbon bonded alumina CFFs.

On the one hand, active coatings present the same chemistry (refers to the phase and crystal structure) with the chemistry of the primary or secondary inclusions, which have to be removed on the surface of carbon-bonded filters. On the other hand, reactive coatings interact with the dissolved oxygen of the steel melt and generate solid inclusions followed by their deposition on the filter surface, which is reported to be considered as an effective solution to reducing the amount of tertiary and also quaternary inclusions [19].

Many studies were aimed to investigate the effectiveness of different oxide ceramic coating materials such as alumina, magnesia, mullite, and spinel on $Al_2O_3$-C filters. In all cases, coated filters have shown better performance than uncoated ones. These studies were focused on removing alumina inclusions from 42CrMo4 high-strength structural steel. Nevertheless, all possible combinations of aluminum and oxygen, hercynite $FeAl_2O_4$ for instance, can be locally formed simultaneously by the introduction of aluminum into steel melt. Hercynite inclusions indeed are formed in the steel melt in the areas with lower dissolved aluminum and higher dissolved oxygen concentrations [20]. These inclusions are formed in local equilibrium conditions in the steel melt with high oxygen concentrations. Due to their high adhesion to the melt, their removal from the melt during ladle metallurgy treatments or casting is complicated [21-22].

In order to determine the reactions taking place during filtration, hercynite coating is applied on $Al_2O_3$-C filters, sintered, and impinged by an Al-killed 304 low carbon stainless steel melt at 1650°C due to the possibility of easier generation of hercynite inclusions in low carbon steels than structural ones. In comparison to the aforementioned coating materials, hercynite consist of iron, which is assumed to exert a catalytic effect on the interactions between refractory and molten steel that can be assumed to accelerate the inclusion deposition rate.

## 2. Experimental Procedure

### 2.1 Materials

The raw materials selected to produce hercynite coated $Al_2O_3$-C filter were the reactive alumina PFR20 (99.83 wt% $Al_2O_3$, 0.05 wt% $Na_2O$, $d_{50}$ 2μm and $d_{90}$ 4 μm, Alteo, France), fine natural graphite (98.5 wt% C, <45μm, Qingdao Xinghe Graphite, China), carbon black powder Printon 125 (75-80 $m^2/g$, Farayand Powder Alvan, Iran), Carbores P (Rütgers, Germany), nano-$TiO_2$ (anatase, 99+%, 10-25 nm, US Research Nanomaterials, USA). Moreover, fused hercynite (55.0 wt.% $Al_2O_3$, 43.0 wt.% $Fe_2O_3$, 0.7 wt.% $SiO_2$, 0.15 wt.% CaO, <45μm, Kaifeng Hecheng Special Refractories, China) used to make the active ceramic coating on the sintered filter surfaces. In addition, the Castament FS65 dispersant (BASF, Germany), Dopalix PC75 dispersant (Zschimmer & Schwarz, Germany), Magnesium Lignosulfonate temporary binder (Borregaard Lignotech, South Africa), Monohydrate citric acid (Industrial food grade, Arrowchem, China) dispersant, and Triton X-100 wetting agent (Daejung, South Korea) were used as additives.

## 2.2 Sample preparation

For the evaluation of the filtration efficiency of hercynite functional coating on carbon-bonded alumina foam filter, $Al_2O_3$-C foam filters were prepared based on an optimum composition containing 1 wt.% of nano-$TiO_2$, which was selected from our previous study where the preparation technique used to process the $Al_2O_3$-C filter composition containing nanomaterials are explored in detail [23]. In this way, $Al_2O_3$-C foam filters and the following hercynite coating were prepared based on the compositions shown in Table 1. To this aim, ceramic foam filters were prepared according to the replica technique patented by Schwarzwalder [24] in the following steps.

1) 10 ppi[1] polyurethane foams ($50\times50\times20$ mm$^3$) were dipped into highly viscose impregnation slurry.

2) Extra slurry was squeezed out from the polymeric sponge by passing through a manual roll pressing device (roller diameter: 44 mm, 4 mm gap between rollers, 60 rpm[2]).

3) Roll pressed foams were kept at ambient temperature for 24 h to get rid of moisture; then, sintered at 800°C under a petroleum coke bed following the heat treatment curve shown in Figure 1.

4) Sintered filters were afterward dipped into a secondary slurry with lower viscosity in comparison to the primary slurry. After 5 seconds (the time was found experimentally), the extra slurry was removed from filters using a compressed air blow gun (nozzle diameter: 5 mm, line pressure: 5 bar, distance between the nozzle tip and the filter: 15 cm).

5) Filters were kept at ambient temperature for 24 h to get rid of moisture; then, sintered at 800°C following the 3rd step.

6) Sintered filters were subsequently dipped into hercynite coating slurry for 10 seconds (the time was found experimentally); then, extra slurry was removed from filters following the 5th step.

7) Filters were kept at ambient temperature for 24 h to get rid of moisture; then, sintered at 1200°C under a petroleum coke bed following the heat treatment curve shown in Figure 1.

**Table 1.** Optimum composition used to prepare foam filters.

| | Composition | | |
|---|---|---|---|
| Raw Material | IS$^{\times}$ | LVIS• | HCS♦ |
| Reactive alumina (wt.%) | 65 | 65 | - |
| Natural fine graphite (wt.%) | 8 | 8 | - |
| Carbon black (wt.%) | 6 | 6 | - |
| Carbores® P (wt.%) | 20 | 20 | - |
| Nano-$TiO_2$ (wt.%) | 1 | 1 | - |
| Fused hercynite (wt.%) | - | - | 100 |
| $^+$Castament FS65 (wt.%) | 0.3 | 0.3 | - |
| $^+$Magnesium lingo sulfunate (wt.%) | 1.5 | 1.5 | 1.5 |
| $^+$ Triton X-100 (wt.%) | 0.2 | 0.2 | - |
| $^+$ Monohydrate citric acid (wt.%) | 0.8 | 0.8 | - |
| $^+$ Dolapix PC75 (wt.%) | - | - | 0.5 |
| $^+$ Dionized water (wt.%) | 20 | 31 | 14 |

$^+$ Related to solid matter content
$^{\times}$ Impregnation slurry
• Lower viscosity impregnation slurry
♦ Hercynite coating slurry

---

[1] Pore per inch
[2] Revolutions per minute

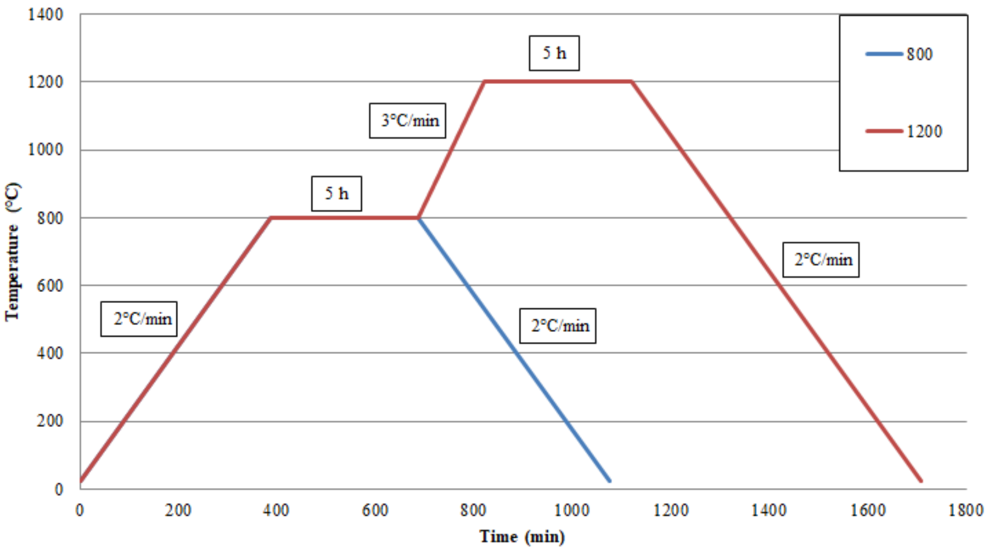

**Fig. 1.** Firing curve of $Al_2O_3$-C foam filters at 800°C and 1200°C.

**Table 2.** Chemical analysis of used steel.

| Element | wt.% |
|---|---|
| C | 0.07 |
| Mn | 1.87 |
| P | 0.038 |
| S | 0.018 |
| Si | 0.32 |
| Al | 0.021 |
| Cr | 18.46 |
| Ni | 8.30 |
| Mo | 0.34 |
| Fe | 69.76 |

## 2.3 Molten steel impingement test

Hercynite coated filters were exposed to the molten Al-killed 304 low carbon stainless steel, where the chemical analysis of the steel is shown in Table 2. To this respect, special casting molds were made using silica sand. The filters were placed in the molds and preheated up to 500°C; afterward, filters were exposed to the molten Al-killed steel with an approximate temperature of 1650°C in three different states, which can be seen in Figure 2.

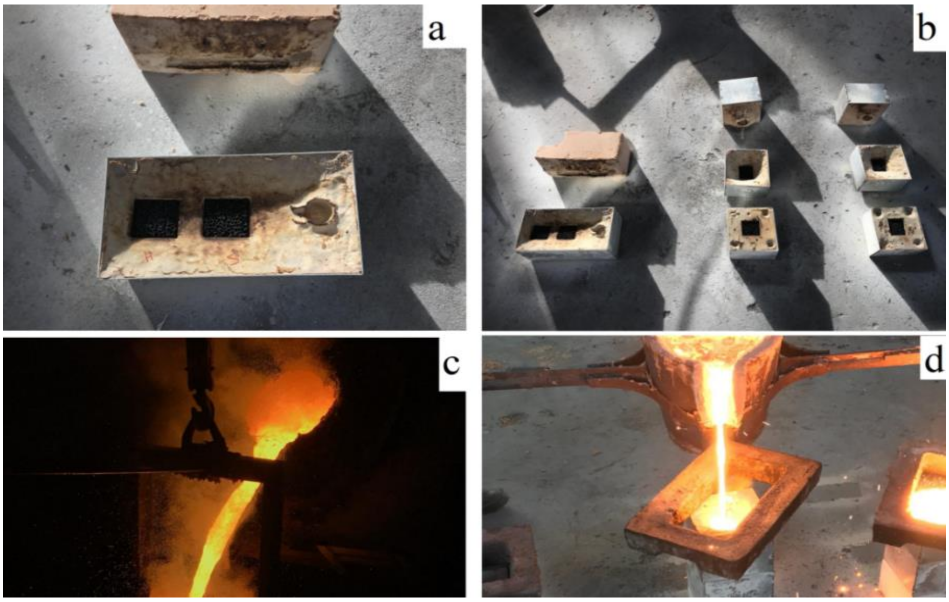

**Fig. 2.** Different stages of the molten steel impingement through $Al_2O_3$-C foam filters with active hercynite coating; filter preparation for the test (a and b), molten steel tapping to the main ladle with an approximate temperature of 1650°C; then, transfer of the molten steel to the casting ladle with an approximate capacity of 50 kg to add aluminum as steel de-oxidizer (c), Al-killed steel casting to the molds (d).

A different amount of aluminum was added to the steel melt to change the oxygen activity of the melt as follows:

1) Addition of normal amount of Al for the steel de-oxidation (0.05 kg Al to 50 kg steel melt) in order to make normal oxygen activity condition

2) Addition of a higher amount of Al than the normal amount for the steel de-oxidation (0.1 kg Al to 50 kg steel melt) in order to make high aluminum activity condition

3) Addition of lower amount of Al than the normal amount for the steel de-oxidation (0.02 kg Al to 50 kg steel melt) in order to make high oxygen activity condition

The filters were released from the molds after 12 h and sent for microstructural investigations.

### 2.4 Microstructural evaluations

Microstructures of the cut surfaces of the filters were evaluated by a scanning electron microscope (FESEM, MIRA3, TESCAN, Czech Republic) equipped with an EDS detector (SAMx SDD, SAMx NumeriX, France).

## 3. Results and Discussion

Active hercynite-coated $Al_2O_3$-C filters were successfully produced by using the replica method. The microstructure of the hercynite coated $Al_2O_3$-C filter before exposure to the steel melt is shown in Figure 3.

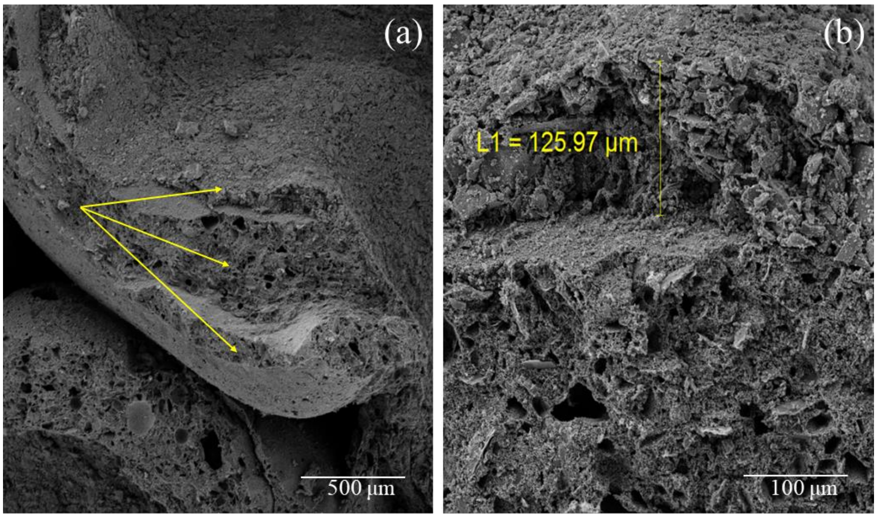

**Fig. 3.** SEM micrographs of filter surface before exposure to the steel melt; a) hercynite coating on the filter strut, b) thickness of applied hercynite coating on the filter surface.

As shown in Figure 3a, three layers of materials could be distinguished from the micrograph, which corresponds to the production process of filters consisting of three different steps. In addition, according to the filter production procedure, the third layer, which has the lowest thickness, must be the hercynite coating. Moreover, one can see from Figure 3b that the layer thickness estimated to be about 125 µm that might differ from one area to another.

The filters were exposed to the steel melt in three different states. In the first scenario, the filter exposed to the steel melt, which had normal oxygen activity conditions, resulted from the addition of a usual amount of aluminum pigs to the steel. It can be seen from the SEM micrographs of Figure 4 that some whiskers were entrapped on the surface of the filter, which can be considered as a hercynite layer, as discussed in the previous paragraph. Additionally, in Figure 5, which presents the SEM micrograph of the filter exposed by the steel melt in high aluminum activity conditions, similar behavior has been detected. The entrapment of dendritic inclusions from the steel melt and the formed whiskers are obvious. Taking the EDS analyses revealed in both Figure 4c and 5c, Al, O, Fe, and C elements were present in both dendritic inclusions and whiskers.

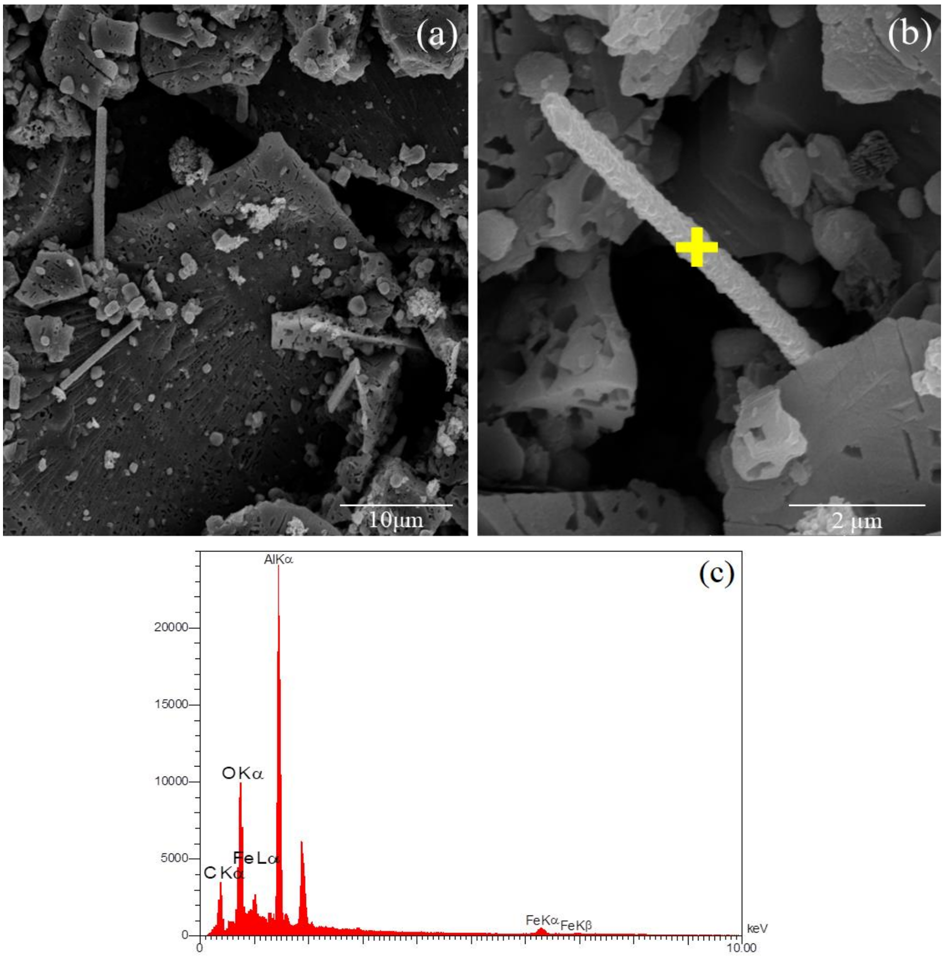

**Fig. 4.** a) and b) SEM micrographs of filter surface after exposure to the steel melt in normal oxygen activity state reveal the formation of corundum whiskers between particles of the hercynite coating; c) EDS analysis of the formed whisker marked in part b.

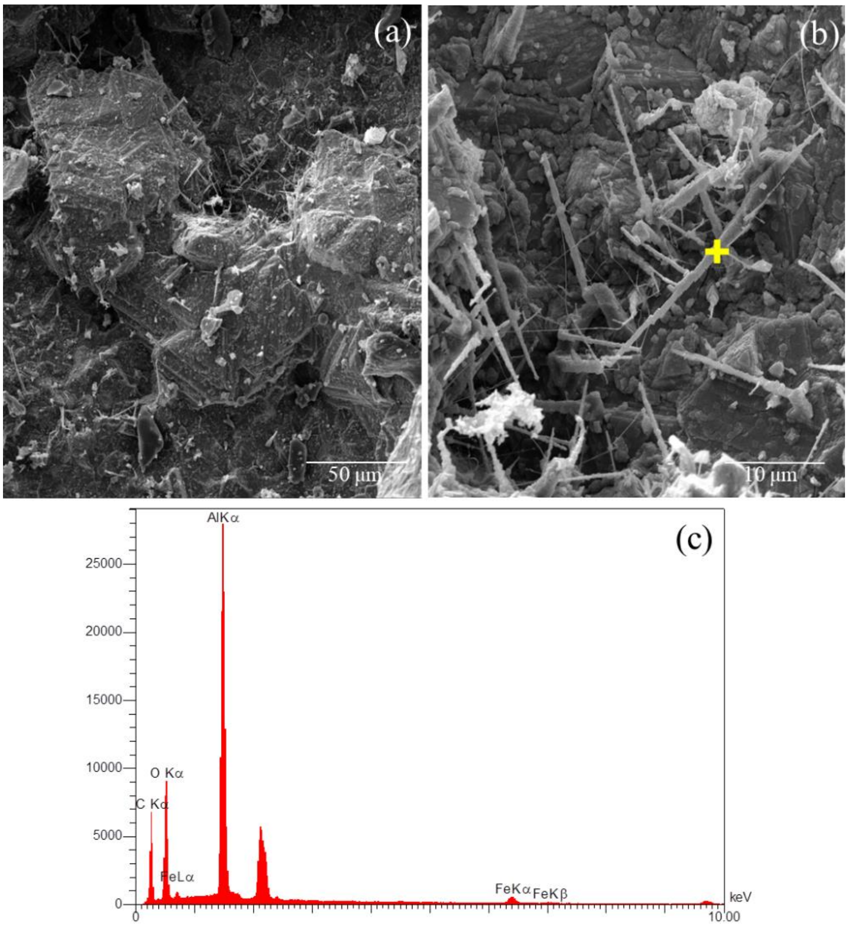

**Fig. 5.** SEM micrographs of the filter surface after exposure to the steel melt in high aluminum activity state reveal the entrapment of dendritic alumina inclusions from the steel melt as well as the formation of alumina whiskers on the surface of the filter; a) and b) reveal different magnifications of the same concept; c) EDS analysis of the formed whisker marked in part b.

Lately, some researchers were investigated the phenomenon of whiskers formation in $Al_2O_3$-C refractories in the $Al_2O_3$-C-Fe system [25], which also were reported by other researchers in the past [26-27]; in fact, based on microstructural investigations and thermodynamic simulations, they have presented the $Al_2O_3$-C whicker formation phenomena in the following order:

a) Strong reduction in the oxygen partial pressure by carbon

b) Formation of Al-containing gas species (Al, $Al_2O$, and AlO) at very low $Po_2$ conditions and solid $Al_4C_3$ and $Al_4O_4C$ with some increase in partial $O_2$ pressure at high temperatures as 1898 K and beyond.

c) Formation of $Al_2O_3$ whiskers and solid carbon on cooling due to the oxidation of gaseous Al-containing species and solid $Al_4C_3$ and $Al_4O_4C$ phases at low temperatures as 1273 K by the reaction with CO gas (in this condition, CO can act as oxidizer atmosphere based on the literature calculations)

Considering their achievements and previous report on $Al_2O_3$-C filter steel/filter interactions [28], the formation of gaseous Al-containing phases and CO gas will take place through carbothermic reduction of $Al_2O_3$ in the filter skeleton under the hercynite coating at both normal oxygen and high Al activity conditions. In the first case, during cooling on the filter surface, the oxidation of Al-containing gaseous species or solid aluminum carbide/oxycarbide phases by CO gas resulting in the formation of $Al_2O_3$ whiskers and solid carbon. In the second case, in addition to the phenomenon that happened in the first condition, because of high Al activity in the steel melt, generated CO gas can be dissolved in the melt through Equation 1 [29].

$CO_{(g)} \rightleftarrows [C] + [O]$ (Eq. 1)

Afterward, high concentration of dissolved Al in the steel melt led to the formation of dendritic $Al_2O_3$ inclusions through Equation 2 on the filter/melt interface and their following adhesion on the filter surface.

$2[Al] + 3[O] \rightleftarrows Al_2O_{3(s)}$ (Eq. 2)

Formation of dendritic $Al_2O_3$ inclusions in high dissolved Al concentrations in the steel melt were previously reported by Steinmetz et al. [30-31] and Okohira et al. [32].

Unlike aforementioned conditions, in the case of high oxygen activity, which was resulted by lower addition of aluminum pigs to the steel melt, the oxygen partial pressure was high enough to inhibit whisker formation resulted in a big change in the morphology of inclusions; in fact, the morphology of the inclusions in the steel melt was shifted to globular, and their sizes were reduced which is shown in Figure 6a and b.

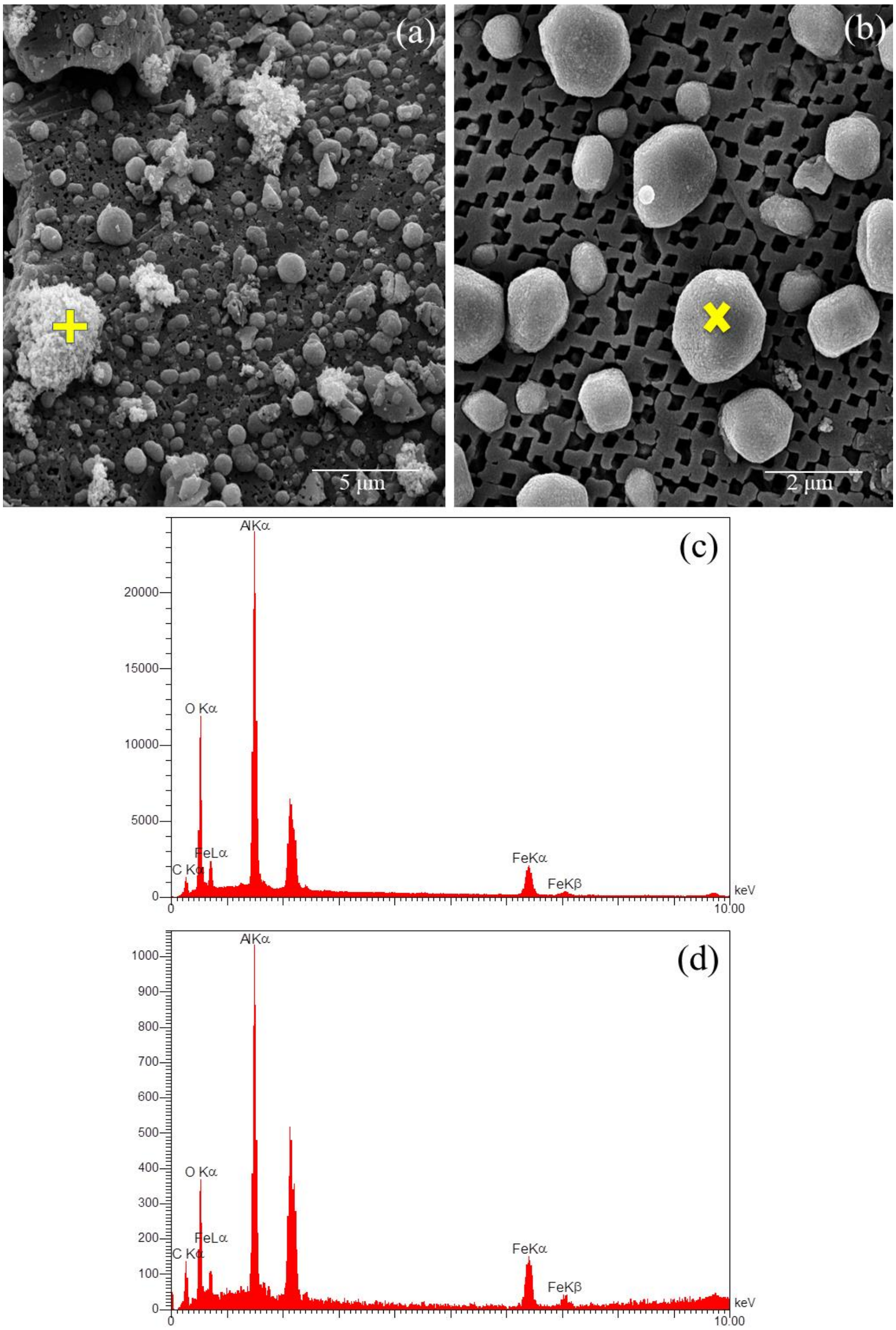

**Fig. 6.** SEM micrographs of the filter surface after exposure to the steel melt in high oxygen activity state reveal the entrapment of hercynite inclusions from the steel melt; a and b reveal different magnifications of the same concept; c and d) EDS analyses of the marked points in part a and b, respectively.

Regarding the presence of O, Al, and Fe elements in the EDS analyses presented in Figures 6c and d, and considering the achievements from Steinmetz et al. [30], the formation of hercynite inclusions in the steel melt and their following entrapment by hercynite coated $Al_2O_3$-C filter were confirmed. In this way, a schematic illustration of the aforementioned filtration phenomena of hercynite coated alumina-carbon filters in different Al/Oxygen activity conditions is shown in Figure 7 for a better understanding.

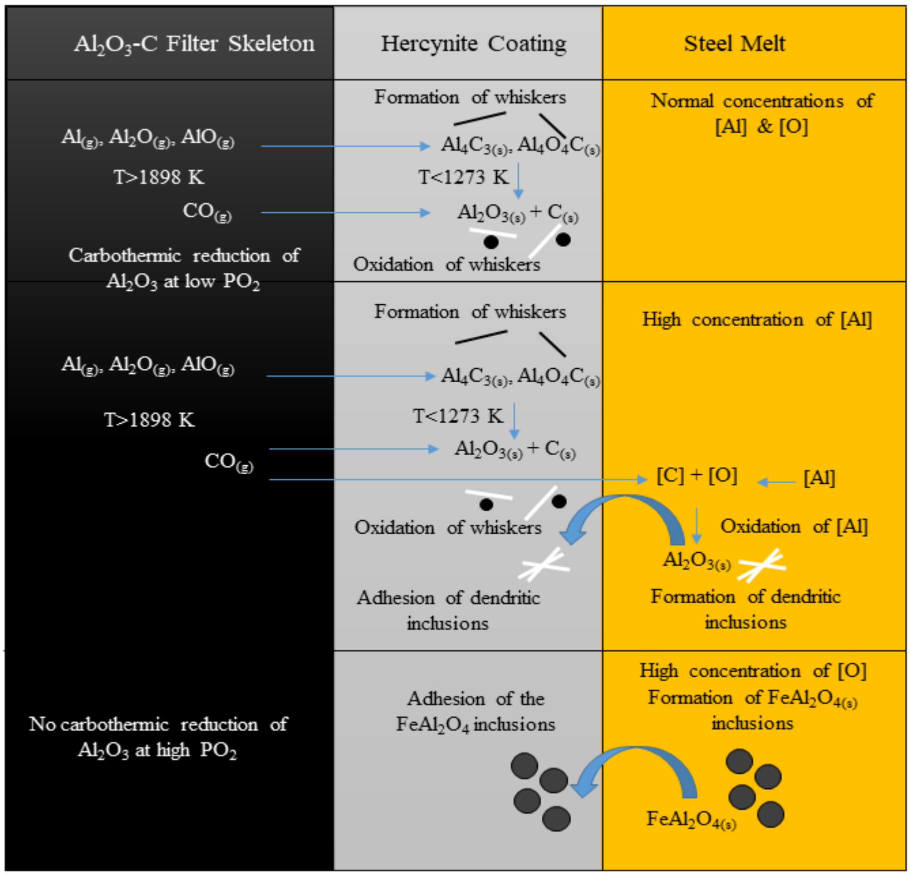

**Fig. 7.** Schematic illustration of the filtration phenomena of hercynite coated $Al_2O_3$-C filters in three different Al/Oxygen concentrations.

Changing the filter surface chemistry by applying the hercynite coating increased the wettability of the filter surface by hercynite inclusions and accelerated the inclusions entrapment. In fact, at high oxygen activity conditions for which can be seen in low and ultra-low carbon steels, a promising application of hercynite coated $Al_2O_3$-C filters in steel casting can be considered.

## 4. Conclusion

In this paper, the filtration mechanism of hercynite coated $Al_2O_3$-C filter by means of a small impingement test in different Al/Oxygen activity conditions and following microstructural investigations were evaluated.

The results indicated that the formation of $Al_2O_3$ whiskers and solid carbon on the surface of the filter takes place through the oxidation of Al-containing gaseous species or solid aluminum carbide/ oxycarbide phases by CO gas at normal oxygen activity conditions of the steel melt. Moreover, adhesion of dendritic $Al_2O_3$ inclusions from the steel melt and formation of $Al_2O_3$ whiskers and solid carbon occurs on the surface of the filter at high Al activity conditions of the steel melt. Besides, hercynite inclusions are formed in the steel melt at high oxygen activity conditions of the steel melt and entrapped by a hercynite-coated $Al_2O_3$-C filter.

Applying the hercynite coating on the surface $Al_2O_3$-C of filters can change the surface chemistry and increase the wettability by hercynite inclusions which can form in low and ultra-low carbon steel melts and then accelerate the inclusions entrapment. This type of ceramic foam filter can have the feasible potential for application in low and ultra-low carbon steel casting processes.

## 5. Acknowledgements

The authors would like to express their sincere gratitude to the Najafabad Branch, Islamic Azad University for the supports of this research.

## 6. References

[1] D. Krewerth, T. Lippmann, A. Weidner, H. Biermann, "Influence of non-metallic inclusions on fatigue life in the very high cycle fatigue regime", Int. J. Fatigue, Vol. 84, 2016, pp. 40-52. https://doi.org/10.1016/j.ijfatigue.2015.11.001

[2] O.A. Shevtsova, N.A. Zyuban, D.V. Rutskii, "Aspects of the formation of sulfide inclusions and their effect on the quality of low-alloy structural steels", Metallurgist, Vol. 54, 2011, pp. 839-844. https://doi.org/10.1007/s11015-011-9382-x

[3] Y. Murakami, S. Beretta, "Small defects and inhomogeneities in fatigue strength: experiments, models and statistical implications", Extremes, Vol. 2, No. 2, 1999, pp. 123-147. https://doi.org/10.1023/A:1009976418553

[4] V.S. Dub, A.A. Safronov, M.A. Movchan, A.V. Ioffe, V.I. Tazetdinov, G.A. Zhivykh, "Effect of a secondary metallurgy technology on the types of forming nonmetallic inclusions and the corrosion resistance of steel", Russ. Metall., Vol. 12, 2016, pp. 1135-1144. https://doi.org/10.1134/S0036029516120077

[5] L. Zhang, "Nucleation, Growth, Transport, and Entrapment of Inclusions During Steel Casting Journal of The Minerals", Metals & Materials Society, Vol. 65, 2013, pp. 1138-1144. https://doi.org/10.1007/s11837-013-0688-y

[6] J. Brockmeyer, L. Aubrey, "Application of ceramic foam filters in molten metal filtration", In: Smothers WJ, ed. Appl. Ref. Ceram. Eng. Sci. Proc. 8. Westerville, Ohio: The American Ceramic Society, 1987; p.63-74.

[7] C.G. Aneziris, A. Ansorge, H. Jaunich, "New approaches of carbon bonded foam filters for filtration of large castings", Ceram. Forum Int., Vol. 85, No. 10, 2008, pp. 100-103.

[8] J. Luyten, S. Mullens, J. Cooymans, A.M. De Wilde, I. Thijs, R. Kemps, "Different methods to synthesize ceramic foams", J. Eur. Ceram. Soc., Vol. 29, No. 5, 2009, pp. 829-832. https://doi.org/10.1016/j.jeurceramsoc.2008.07.039

[9] T. Schlordt, S. Schwanke, F. Keppner, T. Fey, N. Travitzky, P. Greil, "Robocasting of alumina hollow filament lattice structures", J. Eur. Ceram. Soc., Vol. 33, 2013, pp. 3243-3248. https://doi.org/10.1016/j.jeurceramsoc.2013.06.001

[10] P. Colombo, "Conventional and novel processing methods for cellular ceramics", Philosophical Transactions of Royal Society A, Vol. 364, 2006, pp. 109-124. https://doi.org/10.1098/rsta.2005.1683

[11] S. Ali, D. Apelian, R. Mutharasan, "Refining of aluminum and steel melts by the use of multicellular extruded ceramic filters", Can. Metall. Q., Vol. 24, No. 4, 1985, pp. 311-318. https://doi.org/10.1179/cmq.1985.24.4.311

[12] Z. Taslicukur, C. Balaban, N. Kuskonmaz, "Production of ceramic foam filters for molten metal filtration using expanded polystyrene", J. Eur. Ceram. Soc., Vol. 27, 2007, pp. 637-640. https://doi.org/10.1016/j.jeurceramsoc.2006.04.129

[13] C.G. Aneziris, "Clean steel technologies based on interactions of refractory filtering materials with steel melt", J. China's Ref., Vol. 25, No. 3, 2016, pp. 1-10.

[14] M. Emmel, C.G. Aneziris, "Development of novel carbon bonded filter compositions for steel melt filtration", Ceram. Int., Vol. 38, No. 6, 2012, pp. 5165-5173. https://doi.org/10.1016/j.ceramint.2012.03.022

[15] M. Emmel, C.G. Aneziris, G. Schmidt, D. Krewerth, H. Biermann, "Influence of the chemistry of surface functionalized ceramic foam filters on the filtration of alumina inclusions in steel melts", Adv. Eng. Mater., Vol. 15, No. 12, 2013, pp. 1188-1196. https://doi.org/10.1002/adem.201300118

[16] E. Storti, M. Emmel, S. Dudczig, P. Colombo, C.G. Aneziris, "Development of multi-walled carbon nanotubes-based coatings on carbon-bonded alumina filters for steel melt filtration", J. Eur. Ceram. Soc., Vol. 35, No. 5, 2015, pp. 1569-1580. https://doi.org/10.1016/j.jeurceramsoc.2014.11.026

[17] E. Storti, S. Dudcziga, G. Schmidt, P. Colombo, C.G. Aneziris, "Short-time performance of MWCNTs-coated $Al_2O_3$-C filters in a steel melt", J. Eur. Ceram. Soc., Vol. 36, No. 3, 2016, pp. 857-866. https://doi.org/10.1016/j.jeurceramsoc.2015.10.036

[18] M. Emmel, C.G. Aneziris, F. Sponza, S. Dudczig, P. Colombo, "In situ spinel formation in $Al_2O_3$-MgO-C filter materials for steel melt filtration", Ceram. Int., Vol. 40, No. 8, 2014, pp. 13507-13513. https://doi.org/10.1016/j.ceramint.2014.05.033

[19] S. Dudczig, C.G. Aneziris, M. Emmel, G. Schmidt, J. Hubalkova, H. Berek, "Characterization of carbon bonded alumina filters with active or reactive coatings in a steel casting simulator", Ceramics International, Vol. 40, 2014, pp. 16727-16742. https://doi.org/10.1016/j.ceramint.2014.08.038

[20] R. Dekkers, Non-metallic inclusions in Steel, Ph.D. thesis, University of Leuven, 2002.

[21] A. Kazakov, P. Kovalev, S. Ryaboshu, "Metallurgical expertise as the base for determination of nature of defects in metal products", CIS Iron and Steel Review, Vol. 1, No. 2, 2007, pp. 7-13. https://doi.org/10.13140/RG.2.1.4675.3688

[22] P.K. Kovalev, "Improving production technology of tube Steel grades in converter process", Metalurgija, Vol. 55, No. 4, 2016, pp. 715-718.

[23] A. Baghaei, A.A. Nourbakhsh, R. Ebrahimi Kahrizsangi, V.R. Salvini, "Correlation of microstructure and mechanical properties of $Al_2O_3$-C bodies containing Nano-$Al_2O_3$ and Nano-$TiO_2$ additives", International Journal of Applied Ceramic Technology, Vol. 17, No. 3, 2020, pp. 1505-1513. https://doi.org/10.1111/ijac.13435

[24] K. Schwartzwalder, Method of making porous ceramic article, Patent US 3,090,094, 1963.

[25] X. Wei, A. Yehorov, E. Storti, S. Dudczig, O. Fabrichnaya, C. G. Aneziris, O. Volkova, "Phenomenon of whiskers formation in $Al_2O_3$-C refractories" Advanced Engineering Materials, 2021, 2100718. https://doi.org/10.1002/adem.202100718

[26] R. Khanna, M. Ikram-Ul Haq, Y. Wang, S. Seetharaman, V. Sahajwalla, "Chemical interactions of alumina-carbon refractories with molten steel at 1823 K (1550°C): implications for refractory degradation and steel quality", Metallurgical and Materials Transactions B, Vol. 42, 2011, pp. 677-684. https://doi.org/10.1007/s11663-011-9520-7

[27] R. Khanna, S. Kongkarat, S. Seetharaman, V. Sahajealla, "Carbothermic reduction of Alumina at 1823 K in the presence of molten steel: a sessile drop investigation", ISIJ International, Vol. 52, 2012, pp. 992-999. https://doi.org/10.2355/isijinternational.52.992

[28] E. Storti, R. Jankovský, D. Sedmidubský, S. Dudczig, CG. Aneziris, "Filter coatings based on combination of nanomaterials for Steel melt filtration", Advanced Engineering Materials, Vol. 22, 2020, pp. 1900457-64. https://doi.org/10.1002/adem.201900457

[29] JH. Lee, MH. Kang, SK. Kim,YB. Kang, "Oxidation of Ti added ULC steel by CO gas simulating interfacial reaction between the steel and SEN during continuous casting" ISIJ International, Vol.58, 2018, pp. 1257-1266. https://doi.org/10.2355/isijinternational.ISIJINT-2018-164

[30] E. Steinmetz, "Shapes and formation of aluminum oxides in raw ingots and continuously cast slabs", Stahl u. Eisen, Vol.97, 1977, pp. 1154-1159.

[31] E. Steinmetz, HU. Lindenberg, "Morphology of inclusions at aluminum deoxidation", Arch. Eissenhüttenwes, Vol. 47, 1976, pp. 199-204.

[32] K. Okohira, N. Sato, H. Mori, "Observation of three-dimensional shapes of inclusions in low-Carbon Aluminum-killed Steel by scanning Electron microscope", Transactions of the Iron and Steel Institute of Japan, Vol. 14, 1974, pp. 103-109. https://doi.org/10.2355/isijinternational1966.14.102